生 物 工 程 学 报
Chinese Journal of Biotechnology
http://journals.im.ac.cn/cjbcn
DOI: 10.13345/j.cjb.220810

Mar. 25, 2023, 39(3): 1163-1174

·合成生物技术·

基于双工程菌的“锁扣”生物活材料构建及其体内肠道滞留应用

张明慧[1]，张英英[2]，赵鹏程[1]，王汉杰[1*]

1 天津大学生命科学学院，天津 300072
2 徐州医科大学医学影像学院，江苏 徐州 221004

张明慧，张英英，赵鹏程，王汉杰. 基于双工程菌的“锁扣”生物活材料构建及其体内肠道滞留应用[J]. 生物工程学报，2023, 39(3): 1163-1174.
ZHANG Minghui, ZHANG Yingying, ZHAO Pengcheng, WANG Hanjie. Construction of “lock-key” biological living material based on double engineered bacteria and its application on intestinal retention *in vivo*[J]. Chinese Journal of Biotechnology, 2023, 39(3): 1163-1174.

摘　要：生物活材料的研究主要集中在利用单一细菌生产生物膜、水塑料等体外应用。由于菌株尺寸较小，当其应用于体内时，容易发生逃逸，导致滞留效果较差。为解决这一难题，本研究借助大肠杆菌(*Escherichia coli*)表面展示系统(Neae)，在两个菌株表面分别展示 SpyTag 和 SpyCatcher，构建一种双菌“锁扣”型生物活材料生产系统。两菌株之间通过 SpyTag 和 SpyCatcher 的结合，发生原位交联，从而长时间滞留在肠道部位。体外实验表明两菌株混合几分钟后，会发生明显的沉降。此外，利用共聚焦成像和微流控平台进一步证明了该系统在流动状态下的粘附效果。最后，为了验证该系统在体内应用的可行性，小鼠连续 3 d 口服 A 菌(p15A-Neae-SpyTag/sfGFP)和 B 菌(p15A-Neae-SpyCatcher/mCherry)，收集肠道组织进行冷冻切片染色。结果表明，相较于未结合菌株，该双菌系统能更多滞留在小鼠肠道，为生物活材料进一步的体内应用奠定了基础。

关键词：生物活材料；表面展示；SpyTag 与 SpyCatcher；双菌

资助项目：国家重点研发计划(2019YFA0906500)；国家自然科学优秀青年科学基金(32122047)；国家自然科学基金(31971300，81771970)；天津市重点研究与开发计划(19YFZCSY00190)
This work was supported by the National Key Research and Development Program of China (2019YFA0906500), the National Natural Science Foundation of China for Outstanding Young Scientists (32122047), the National Natural Science Foundation of China (31971300, 81771970), and the Key Research and Development Program of Tianjin, China (19YFZCSY00190).
*Corresponding author. E-mail: wanghj@tju.edu.cn
Received: 2022-10-08; Accepted: 2023-01-09; Published online: 2023-01-11

Construction of “lock-key” biological living material based on double engineered bacteria and its application on intestinal retention *in vivo*

ZHANG Minghui[1], ZHANG Yingying[2], ZHAO Pengcheng[1], WANG Hanjie[1*]

1 School of Life Sciences, Tianjin University, Tianjin 300072, China
2 School of Medical Imaging, Xuzhou Medical University, Xuzhou 221004, Jiangsu, China

Abstract: At present, the research of biological living materials mainly focuses on applications *in vitro*, such as using a single bacterial strain to produce biofilm and water plastics. However, due to the small volume of a single strain, it is easy to escape when used *in vivo*, resulting in poor retention. In order to solve this problem, this study used the surface display system (Neae) of *Escherichia coli* to display SpyTag and SpyCatcher on the surface of two strains, respectively, and constructed a double bacteria “lock-key” type biological living material production system. Through this force, the two strains are cross-linked *in situ* to form a grid-like aggregate, which can stay in the intestinal tract for a longer time. The *in vitro* experiment results showed that the two strains would deposit after mixing for several minutes. In addition, confocal imaging and microfluidic platform results further proved the adhesion effect of the dual bacteria system in the flow state. Finally, in order to verify the feasibility of the dual bacteria system *in vivo*, mice were orally administrated by bacteria A (p15A-Neae-SpyTag/sfGFP) and bacteria B (p15A-Neae-SpyCatcher/mCherry) for three consecutive days, and then intestinal tissues were collected for frozen section staining. The *in vivo* results showed that the two bacteria system could be more detained in the intestinal tract of mice compared with the non-combined strains, which laid a foundation for further application of biological living materials *in vivo*.
Keywords: biological living materials; surface display; SpyTag-SpyCatcher; bi-bacteria

传统的生物材料，如无机纳米材料、碳纳米材料、高分子纳米材料以及超分子纳米材料等[1]，在骨修复[2-3]、伤口愈合[4-6]、肿瘤诊治疗[7-9]、成像[8]以及脑疾病治疗[10]等方面应用广泛。但是，其合成过程繁琐，物理结构、表面性质和固有功能难以改变，并且它们在体内应用过程中也出现了无法自主调节、持续时间短等问题。因此，需要开发一种可编程、能够自我调节的新型生物活材料[11]来满足体内应用的各种需求。

近几年，新型生物活材料的研究获得进展，其中生物被膜的研究最为广泛[12-15]。例如，哈佛大学 Neel S. Joshi 教授团队利用生物被膜开发了一种可降解“水塑料”[16]，用于解决日益严重的塑料污染问题。此外，借助环境响应型基因表达开关，科学家们开发了可穿戴生物传感器，从而实现无创、实时健康监测[17-19]。美国马萨诸塞大学研究团队将生物被膜设计成皮肤贴片，通过感知汗液，为可穿戴设备发电[20]。深圳先进技术研究院钟超课题组利用大肠杆菌和枯草芽孢杆菌生物被膜的 CsgA 蛋白来生产用于水下粘合的活体胶水[21-23]；此外，在 CsgA

蛋白表面融合其他功能蛋白，研发用于环境消毒[24]、黏膜修复[25-26]以及生物催化[27]的新型生物活材料。

目前，新型生物活材料的研究集中在利用单一菌株的生物被膜来生产各种功能活材料，并探究其体外应用。研究发现[28]：当单一菌株应用到体内时，其难以在靶部位长时间滞留，容易发生逃逸，导致治疗效果大打折扣。随着合成生物学技术的发展，生物活材料也逐步应用到体内。为了使其更好地在体内发挥作用，需要开发一种能够长时间滞留在体内的生物活材料[29-30]。深圳先进技术研究院戴卓君课题组利用大肠杆菌反向自动转运蛋白和表面展示系统[31-32]，将抗原、抗体分别展示在两个菌株表面，构建一种可原位交联的生物活材料，并将其用于 3D 打印、有机磷农药降解、海藻糖合成和可穿戴生物传感器。考虑到肠道环境的复杂性，本研究采用 SpyTag 和 SpyCatcher 这一更加稳定共价连接系统[33]，将其分别展示在两菌株表面[34]，用于开发一种新型可编程、能在肠道持久滞留的生物活材料。这一活材料在体内外可以稳定地交联成网格状结构，从而使菌株更多、更持久滞留在肠道部位。我们相信这种新型生物活材料为肠道疾病、肿瘤等重大疾病的高效治疗提供新思路。

1 材料与方法

1.1 材料

1.1.1 菌株和质粒

本文所用的菌株和质粒详见表 1。

1.1.2 PCR 引物

本文所用引物如表 2 所示。

1.1.3 试剂和仪器

胰蛋白胨、酵母提取物购自 OXOID 公司；氯化钠和琼脂粉购自北京索莱宝科技有限公司；本文所有引物和 Neae 表面展示基因由金唯智公司合成；氯霉素、硫酸卡那霉素和氨苄青霉素粉末购自北京索莱宝科技有限公司；Prime STAR Max Premix (2×)购自 TaKaRa 公司；重组酶、2×Rapid *Taq* Master Mix、质粒小提试剂盒、纯化试剂盒、DNA Marker 和 10×DNA 上样缓冲液购自南京诺唯赞生物科技股份有限公司；恒温培养摇床购自天津欧诺仪器股份有限公司；电泳仪和 PCR 仪购自伯乐公司；微型注射泵购自深圳市瑞沃德生命科技有限公司；多功能酶标仪购自赛默飞世尔科技公司；共聚焦显微镜购自尼康公司。

1.2 方法

1.2.1 质粒构建

质粒构建按参考文献中所述方法[35]。

表 1 本文所用菌株和质粒

Table 1 Strains and plasmids used in this study

Strain and plasmid	Feature	Source
E. coli DH5α	Cloned strain	In the lab
E. coli BL21	Functional verification	In the lab
pRSF-J23100-sfGFP	Green fluorescent protein tag	In the lab
mCherry	Red fluorescent protein tag	In the lab
p15A-Neae-SpyTag	SpyTag displayed on the bacteria surface	Constructed in this study
p15A-Neae-SpyCatcher	SpyCatcher displayed on the bacteria surface	Constructed in this study
p15A-Neae-SpyTag-SnoopTag	SpyTag and SnoopTag displayed on the surface	Constructed in this study
pUC19-SnoopCatcher	Expressed SnoopCatcher	Constructed in this study

表 2 本研究所用引物

Table 2 PCR primes used in this study

Primer name	Primer sequence (5′→3′)
p15a-gj-tag-f	ATGCATACAAGCCGACGAAGTAATAAAGCCAGGCATCAAATAAAACGAAAGGCTCA
p15a-gj-tag-r	ATATCATGCGGAATATTCAGAGAAAGAATATCCTGCTTCTTGTACTCCAG
p15a-pd-tag-f	CTGAATATTCCGCATGATATTAATGGTACTGAACAC
p15a-pd-tag-r	CTTCGTCGGCTTGTATGCATCAACCATGACAATATGGGCTCTAGTCGCACCATCAAAAAATA TAACCGCA
p15a-gj-SpyCatcher-F	AAGGTGACGCTCATATTGATTAATAAAGCCAGGCATCAAATAAAACGAAAGG
p15a-gj-SpyCatcher-R	GATAAGGTATCAACCATGGCTCTAGTCGCACCATCAAAAAATATAACCGCA
SpyCatcher-F	GCCATGGTTGATACCTTATCAGGTTTATCAAG
YZ-SpyCatcher-R	ATCAATATGAGCGTCACCTTTAGTTGCTT
snoop-spy-gj-F	TTATTATCACTTATTCAGGCGTAGCACCAGGCGTTTAAGGG
snoop-spy-gj-R	TCGCCCAGTTTTCCCATATGACCAGATCCGCCCTTCGTCGGCTTGTATGCATCAAC
SnoopTag-PD-F	CATATGGGAAAACTGGGCGATATTGAATTTATTAAAGTGAACAAATAATAAAGCCAGGCATC AAATAAAACGAAAGG
JP-R-3Tag	GCCTGAATAAGTGATAATAAGCGGATGAATG
SC-GJ-F	TAAAGCGCTGCATGCCTAGTG
SC-GJ-R	CTCTAAACAAAATTATTCATTATACGAGCCGGA
SC-PD-F-2	ATGAATAATTTTGTTTAGAGAAAGAGGAGAAATACTAGATGCATATGAAGC
SC-PD-R-2	ACTAGGCATGCAGCGCTTTAATGATGGTGATGGTGATGTTTCGG

1.2.2 两菌株粘附的验证

将测序正确的 p15A-Neae-SpyTag/sfGFP 和 p15A-Neae-SpyCatcher/mCherry 质粒分别转化到大肠杆菌 BL21 中，构建 A 菌(p15A-Neae-SpyTag/sfGFP)和 B 菌(p15A-Neae-SpyCatcher/mCherry)。随后接种到含氯霉素和氨苄青霉素的液体 LB 培养基，37 ℃过夜培养。第 2 天，按照 1:100 的比例将其接种到 15 mL LB 培养基中，继续培养 24 h。将两菌株等量混合后静置，在不同时间点，收集菌液上清，用多功能酶标仪测定上清 OD_{600} 值的变化。

分别取 2 mL A 菌和 B 菌，在透明的玻璃管中等量混合后静置，在 0、10、60 min 这 3 个时间点进行拍照。

1.2.3 激光共聚焦显微镜观察两菌株粘附

在验证菌株间的交联时，我们设置了 4 组实验，分别是对照组(sfGFP+mCherry、A 菌+mCherry、sfGFP+B 菌)和实验组(A 菌+B 菌)。对于实验组，分别取 10 μL 的 A 菌和 B 菌，先后滴在同一载玻片的相同位置，静置片刻，将盖玻片覆盖在载玻片上。对照组操作同上。利用激光共聚焦显微镜来观察绿色荧光和红色荧光的重叠效果。

1.2.4 p15A-Neae-SpyTag-SnoopTag 和 p15A-Neae-SpyCatcher 粘附的验证

为了进一步验证两菌株的交联，将 p15A-Neae-SpyTag-SnoopTag 和 p15A-Neae-SpyCatcher 质粒分别转化到 BL21 菌株中。按此前同类方法培养，混合静置后，测定上清 OD_{600} 的变化。

1.2.5 SnoopCatcher 蛋白的纯化

将测序正确的 pUC19-SnoopCather 质粒转化到 BL21 菌株中，37 ℃过夜培养。第 2 天，将其接种到 1 L 的 LB 培养基中，37 ℃培养 24 h。4 000 r/min 离心 20 min，收集菌体沉淀。加入裂解液(20 mmol/L Tris, 300 mmol/L NaCl, pH 8.0)重悬菌体，超声破碎 40 min。破碎完成后，18 000 r/min

离心 30 min，收集上清。通过 0.22 μm 滤膜过滤、镍柱纯化，用超滤管对蛋白进行浓缩。

1.2.6 采用微流控芯片技术来验证两菌株的粘附

微流控芯片按文献[36]所述来制作。芯片尺寸为 1 500 mm×500 mm，深度是 100 μm。聚二甲基硅氧烷(polydimethylsiloxane, PDMS)层与玻璃片键合之前，先对玻璃片进行活化。活化的玻璃片经烷化处理，被修饰上氨基。通过氨基-羧基之间的共价结合反应，SnoopCatcher 蛋白成功结合到微流控芯片上。A 菌以 40 μL/min 流速流通 3 h。随后，将去离子水以 20 μL/min 的流速来冲洗掉未结合 A 菌。最后，表达 mCherry 的菌株和 B 菌分别以 40 μL/min 流速流通 3 h。利用去离子水冲洗未结合的 mCherry 菌株和 B 菌株，并将其置于激光共聚焦显微镜下观察。

1.2.7 体内粘附效果的验证

将雌性 BALB/c 小鼠随机分成对照组(sfGFP+mCherry)和实验组(A 菌+B 菌)，n=3。对照组小鼠灌胃 200 μL 过夜培养的 sfGFP 菌株，实验组小鼠灌胃 200 μL 过夜培养的 A 菌。1 h 后，对照组小鼠灌胃同等体积的 mCherry 菌株，实验组小鼠灌胃同等体积的 B 菌。连续灌胃 3 d，第 4 天不做任何处理，第 5 天重复此前操作。4 h 后，收集小鼠结肠、空肠、回肠、十二指肠段进行冷冻切片，经 Hoechst 染色后，置于激光共聚焦显微镜下观察。本文动物实验方案遵守相关实验动物福利规定，并获得中国医学科学院放射医学研究所实验动物伦理委员会批准，批准号为 SYXK (津)：2019-0002。

2 结果与分析

2.1 A 菌(p15A-Neae-SpyTag/sfGFP)和 B 菌 (p15A-Neae-SpyCatcher/mCherry) 粘附的验证

肠出血型大肠杆菌的内膜 N 端，是一个反向自动转运蛋白和表面展示系统。基于此，SpyTag 和 SpyCatcher 可展示在两菌株表面(图 1)。将两菌株等量混合，静置。结果显示：静置 10 min 时，约 25%菌株粘附并沉降下来。静置 60 min 后，60%以上菌株明显聚集并沉降(图 2、图 3)。而表面未展示 SpyTag 和 SpyCatcher 的菌株，在所监测的 3 h 内并未发生任何聚集现象(图 3)。

2.2 不同比例 A 菌和 B 菌以及功能性菌株间的粘附

当该双菌系统应用于体内时，双菌数量无法严格控制。因此，我们探究了 A 菌与 B 菌在 1:0.25、1:0.50、1:0.75 比例下的粘附情况。结果表明：随着 B 菌数量的增加，A 菌和 B 菌粘附速率增加(图 4A)。为了增加该双菌系统的功能性，我们引入了一对与 SpyTag-SpyCatcher 正交的共价偶联系统(SnoopTag-SnoopCatcher)，在 p15A-Neae-SpyTag 质粒上延伸出一个 SnoopTag 位点。随后探讨了 SnoopTag 的加入是否会影响粘附效果。结果表明，在最初 30 min 内，

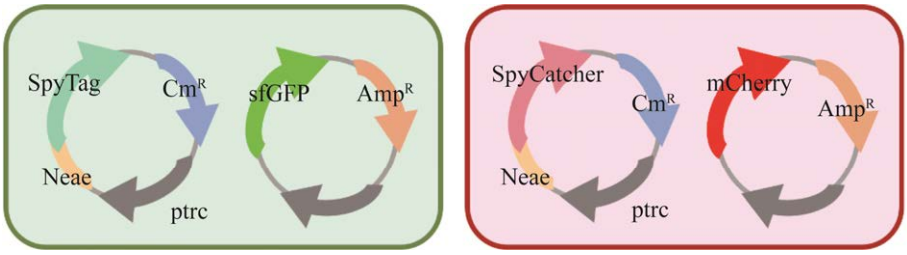

图 1 A 菌(左)和 B 菌(右)质粒构建示意图

Figure 1 The schematic diagram of plasmids of bacteria A (left) and B (right).

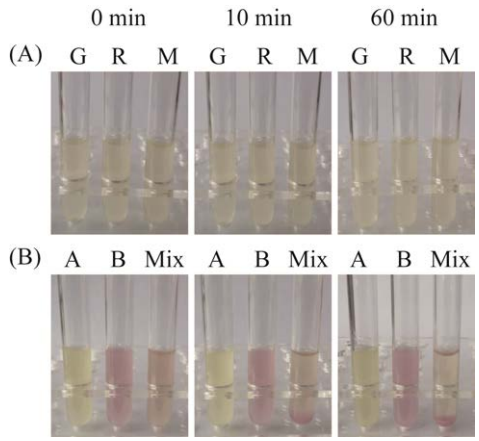

图 2　菌株等量混合的宏观沉降图　(A)：单独表达 sfGFP 和 mCherry 的菌株等量混合后的宏观沉降图. G：sfGFP；R：mCherry；M：sfGFP+mCherry. (B)：A 菌和 B 菌等量混合后的宏观沉降图. A：p15A-Neae-SpyTag/sfGFP；B：p15A-Neae-SpyCatcher/mCherry；Mix：p15A-Neae-SpyTag/sfGFP+p15A-Neae-SpyCatcher/mCherry

Figure 2　Macro sedimentation diagram of equal mixing of strains. (A): Macro-sedimentation diagram of strains separately expressing sfGFP and mCherry mixing in equal amounts. G: sfGFP; R: mCherry; M: sfGFP+mCherry. (B): Macro-sedimentation diagram of macro sedimentation diagram of mixed bacteria A and B in equal amount. A: p15A-Neae-SpyTag/sfGFP; B: p15A-Neae-SpyCatcher/mCherry; Mix: p15A-Neae-SpyTag/sfGFP+p15A-Neae-SpyCatcher/mCherry.

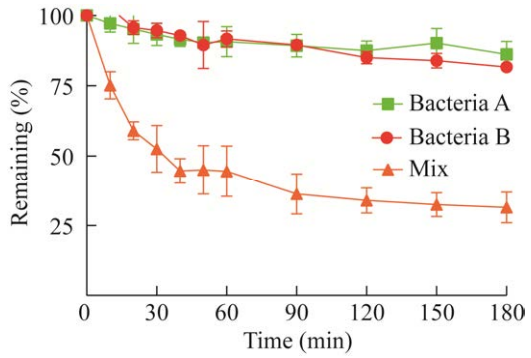

图 3　A 菌和 B 菌粘附的定量验证

Figure 3　Quantitative verification of adherence of bacteria A and B.

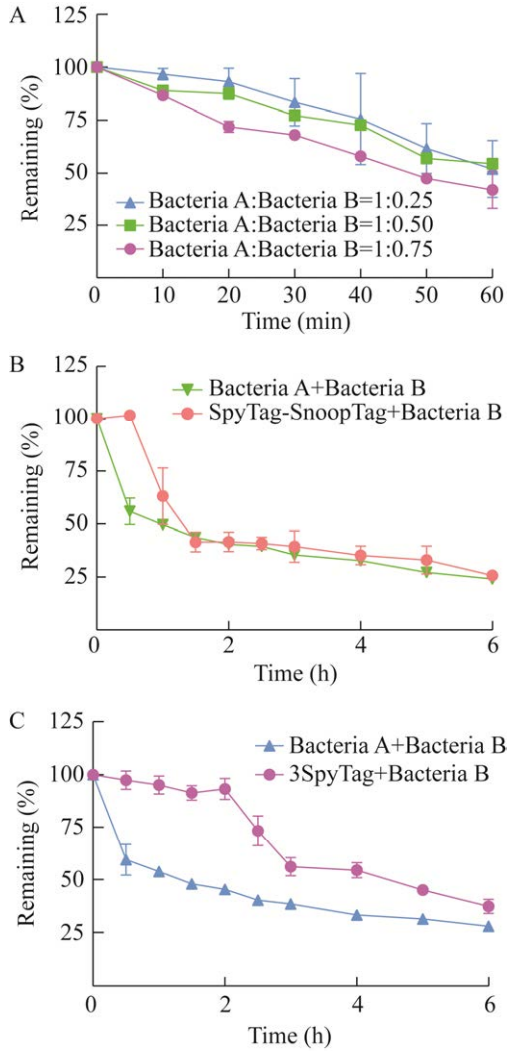

图 4　上清液中剩余的细菌含量　A：不同比例 A 菌和 B 菌混合后，上清中剩余细菌的含量变化. B：p15A-Neae-SpyTag-SnoopTag 菌株与 B 菌混合不同时间后，上清中剩余细菌的含量变化. C：p15A-Neae-3SpyTag 菌株与 B 菌混合不同时间后，上清中剩余细菌的含量变化

Figure 4　Residual bacterial content in the supernatant. A: The content change of residual bacteria in supernatant after mixing bacteria A and B in different proportions. B: The content change of residual bacteria in supernatant after mixing p15A-Neae-SpyTag-SnoopTag strains and bacteria B for different times. C: The content change of residual bacteria in supernatant after mixing p15A-Neae-3SpyTag strains and bacteria B for different times.

p15A-Neae-SpyTag-SnoopTag 菌株与 B 菌粘附效果不明显。随着时间延长，该菌株和 B 菌的粘附与 A、B 两菌的粘附效果类似(图 4B)。最后，我们又尝试了 3 个串联的 SpyTag 展示在 A 菌表面，探究其与 B 菌的粘附效果。结果表明：串联 3 个 SpyTag 不仅影响两菌株粘附速度，粘附效果也大大降低(图 4C)。这可能是由于延伸出的链过长，阻碍了邻近位点结合。

2.3 激光共聚焦显微镜验证 A 菌和 B 菌粘附

除了从宏观角度观察两菌株的粘附外，我们还从微观角度进行了验证。分别将对照组(sfGFP+mCherry、A 菌+mCherry、sfGFP+B 菌)和实验组(A 菌+B 菌)的两菌株混合，并置于低倍镜下观察。如图 5A 所示，与对照组相比，实验组绿色荧光和红色荧光重叠效果较好。将其置于 100 倍油镜下观察，可以更清楚地看到 A 菌和 B 菌的粘附现象(图 5B)。

2.4 微流控平台验证 p15A-Neae-SpyTag-SnoopTag 菌株和 B 菌的粘附

利用微流控平台对 p15A-Neae-SpyTag-SnoopTag 菌株与 B 菌的粘附进行了验证。首先将 SnoopCatcher 蛋白固定在微流控芯片上，通过 SnoopTag-SnoopCatcher 之间的共价结合，将 p15A-Neae-SpyTag-SnoopTag 菌株固定在微流控芯片的指定通道，然后流通 B 菌(图 6A)。与未展示 SpyCatcher 的菌株相比，表面展示 SpyCatcher 的菌株能够更好地与 p15A-Neae-SpyTag-SnoopTag 菌株结合(图 6B)，从而发生粘附。

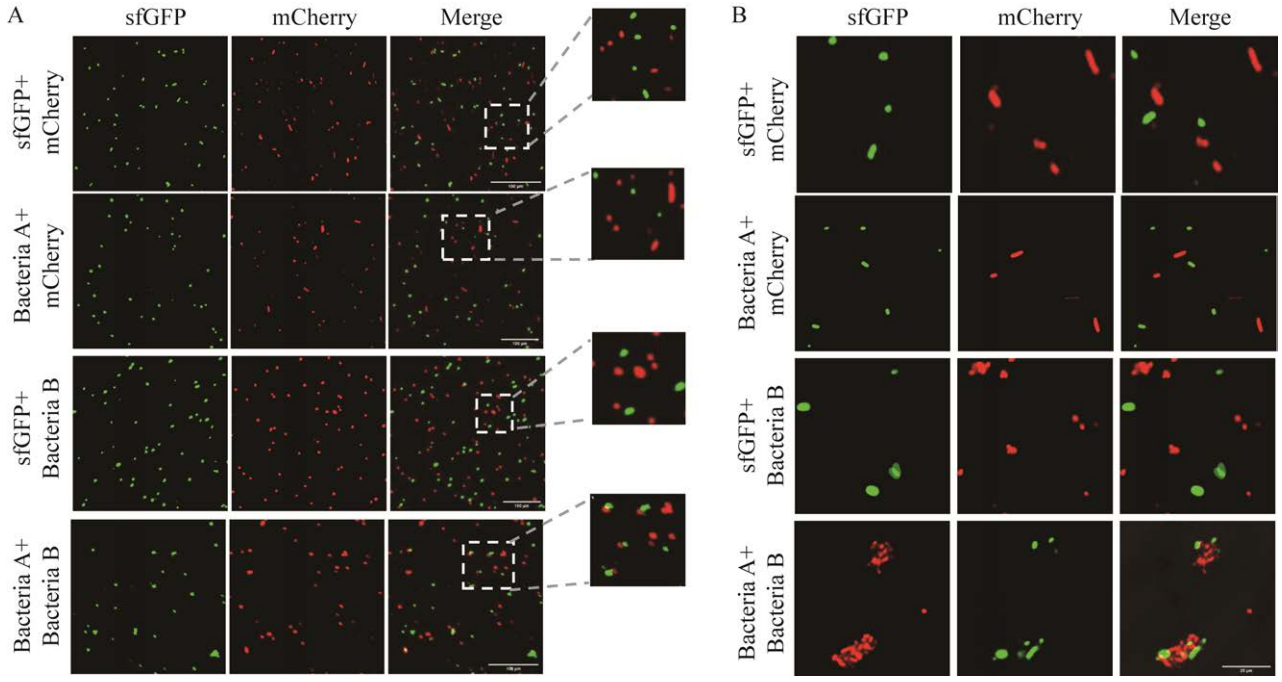

图 5 激光共聚焦显微镜观察菌株的粘附现象 A：在激光共聚焦显微镜 10 倍镜下观察 sfGFP+mCherry、A 菌+mCherry、sfGFP+B 菌、A 菌+B 菌的粘附. B：在激光共聚焦显微镜 100 倍镜下观察 sfGFP+mCherry、A 菌+mCherry、sfGFP+B 菌、A 菌+B 菌的粘附

Figure 5 Observation of bacterial adhesion by laser confocal microscopy. A: The adhesion effects of sfGFP+mCherry, bacteria A+mCherry, sfGFP+bacteria B, and bacteria A+bacteria B were observed under a laser confocal microscope (10×). B: The adhesion effects of sfGFP+mCherry, bacteria A+mCherry, sfGFP+bacteria B, and bacteria A+bacteria B were observed under a laser confocal microscope (100×).

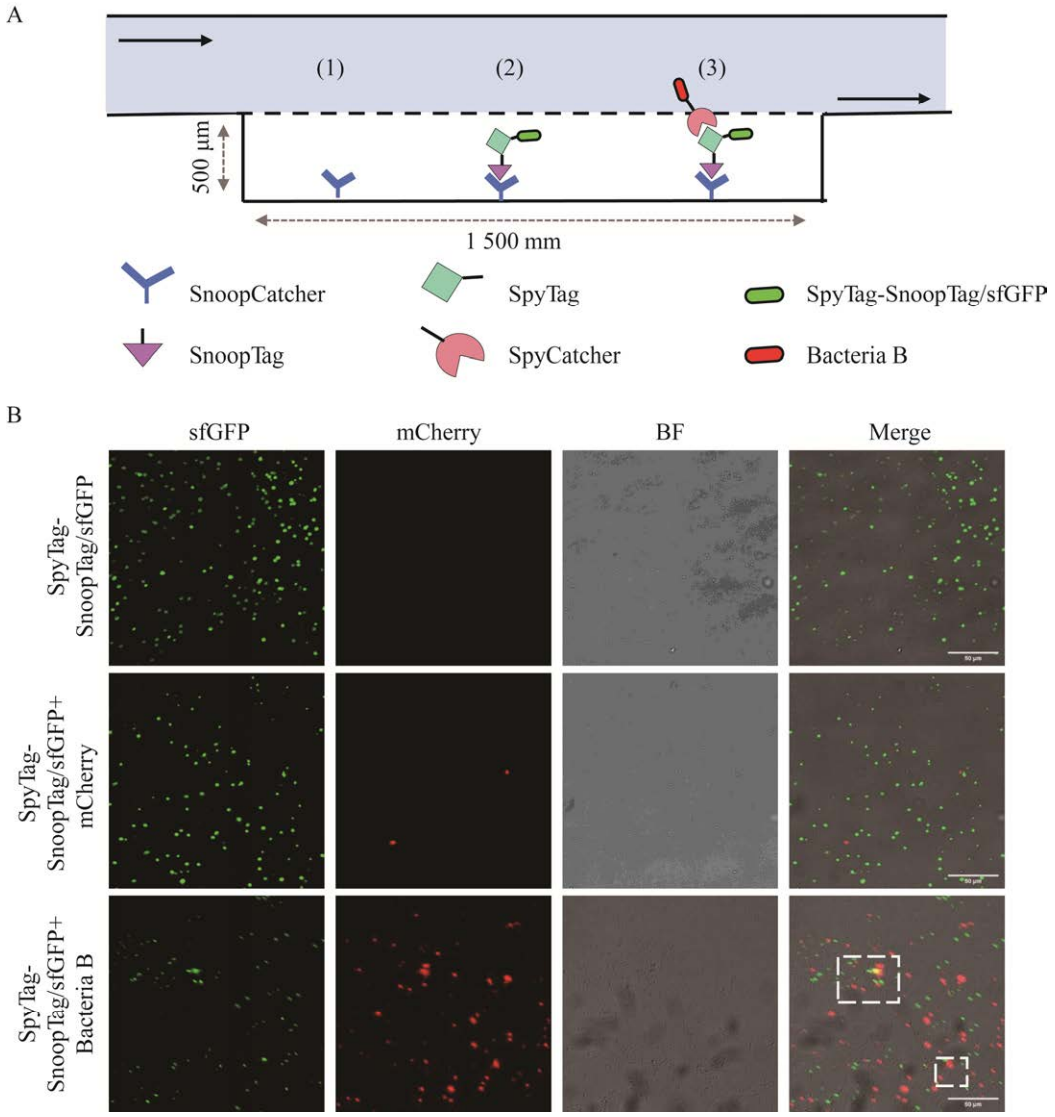

图 6　流动状态下两菌株的粘附　A：微流控操作过程示意图. (1) 先将 SnoopCatcher 蛋白固定在芯片上；(2) 然后流通 p15A-Neae-SpyTag-SnoopTag 菌株；(3) 最后流通 B 菌，使其与 p15A-Neae-SpyTag-SnoopTag 结合. B：显微镜观察 p15A-Neae-SpyTag-SnoopTag 菌株和 B 菌的粘附情况

Figure 6　Adhesion of two strains in flowing state. A: The schematic diagram of microfluidic controlling process. (1) SnoopCatcher protein was fixed on the chip; (2) p15A-Neae-SpyTag-SnoopTag strains were injected; (3) B strains were combined with the previous strain. B: The adhesion of p15A-Neae-SpyTag-SnoopTag strains and bacteria B observed by a laser confocal microscope.

2.5　双菌体系在体内粘附效果的验证

为了验证“锁扣”型生物活材料在体内应用的效果，连续 3 d 先后给小鼠口服 A 菌和 B 菌，在第 5 天收集结肠、空肠、回肠、十二指肠进行冷冻切片，然后置于共聚焦显微镜下观察。结果显示(图 7A)：与单独口服 sfGFP 或 mCherry 菌株相比，A 菌和 B 菌在结肠、空肠和十二指肠的粘附效果更加明显。在回肠部位，两者区别不大。此外，荧光定量分析结果(图 7B)与图 7A 一致。以上结果表明，该双菌体系在肠道内可

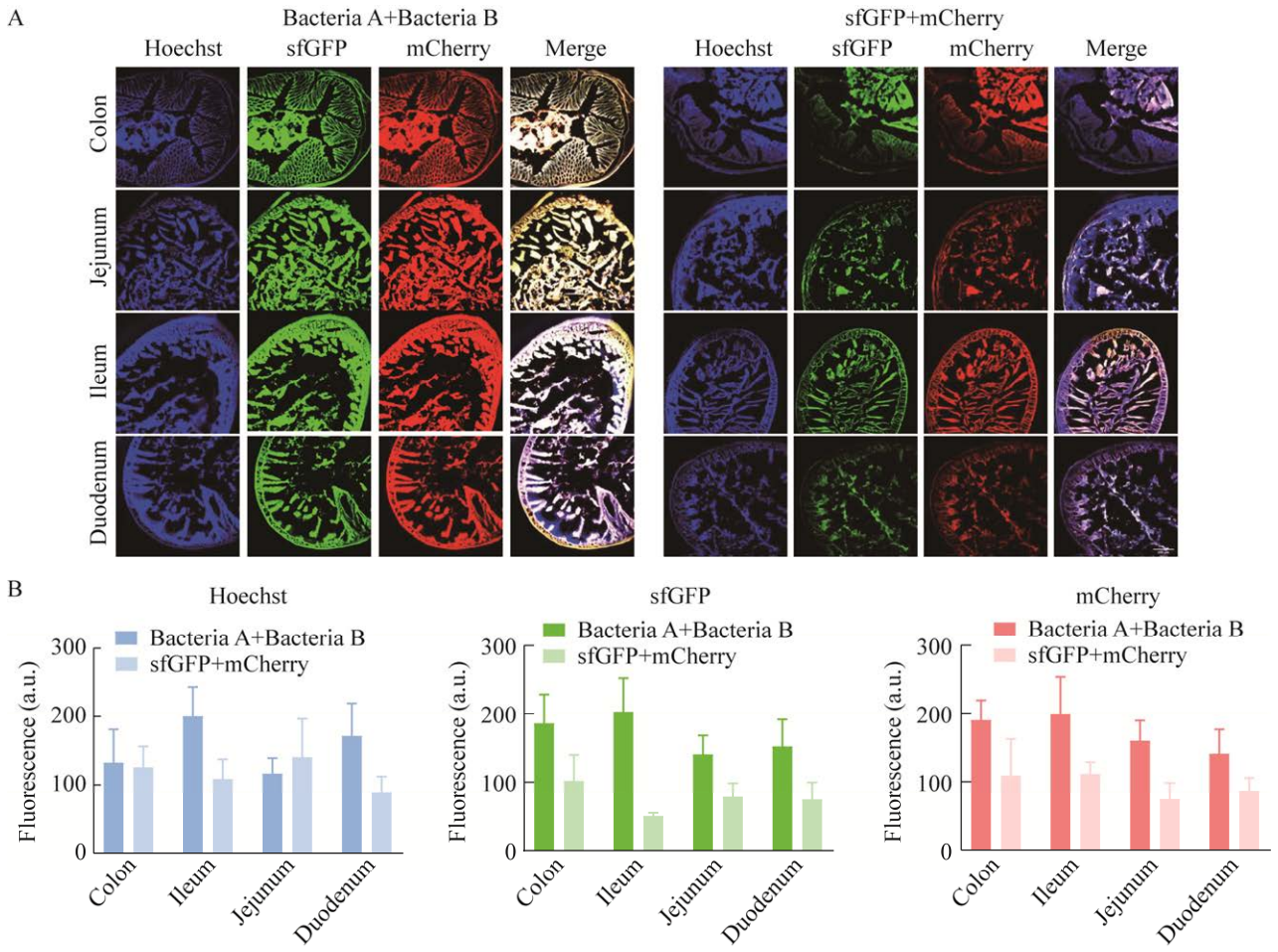

图 7 “锁扣”型生物活材料在肠道内的滞留 A：左边为 A 菌和 B 菌在小鼠不同肠段(结肠、回肠、空肠和十二指肠)的粘附情况；右边为单独的 sfGFP 菌株和 mCherry 菌株在不同肠段的粘附情况. B：图 7A 的荧光强度定量分析(左边：Hoechst 荧光强度定量分析；中间： sfGFP 荧光强度定量分析；右边：mCherry 荧光强度定量分析)

Figure 7 Retention of “lock-key” biological living materials in intestine. A: Left is the adhesion of bacteria A and B in different intestinal segments of mice (colon, ileum, jejunum, and duodenum). Right is the adhesion of individual sfGFP strains and mCherry strains in different intestinal segments. B: Quantitative analysis of fluorescence intensity in Figure 7A. Left: Quantitative analysis of Hoechst fluorescence intensity; Intermediate: Quantitative analysis of sfGFP fluorescence intensity; Right: Quantitative analysis of mCherry fluorescence intensity.

以很好地粘附，并且滞留效果也要优于单一菌株，有效提高了工程菌在肠道的滞留效率，有望在体内得到广泛的应用。

3 讨论

生物活材料的可编程性、持续性以及动态可调性，在其生物医学应用方面具有重要意义。相较于传统的生物材料，生物活材料不仅可以精准到达病灶，减少毒副作用，还可以通过在病灶部位的定植，持久发挥作用。而且，合成生物学技术可以给生物活材料定制不同功能。因此，生物活材料在生物催化、皮肤修复、环

境污染治理、仿生器官[37]以及某些疾病诊疗等方面广泛应用。

截至目前，生物活材料多集中在体外应用。单一菌株在体内发挥作用时，滞留效率低，限制了进一步应用。本研究对微生物进行基因工程改造，利用菌株间的交联形成大的网格状聚集体，能够帮助菌株长久滞留在体内。在后续研究中，可以引入治疗物质，从而拓宽生物活材料的应用范围。本研究可以为新型生物活材料的体内应用提供新的思路。

REFERENCES

[1] ZHAO Y, ZHANG ZZ, PAN Z, LIU Y. Advanced bioactive nanomaterials for biomedical applications[J]. Exploration, 2021, 1(3): 20210089.

[2] CUI ZK, KIM S, BALJON JJ, WU BM, AGHALOO T, LEE M. Microporous methacrylated glycol chitosan-montmorillonite nanocomposite hydrogel for bone tissue engineering[J]. Nature Communications, 2019, 10: 3523.

[3] CUI ZK, KIM S, BALJON JJ, DOROUDGAR M, LAFLEUR M, WU BM, AGHALOO T, LEE M. Design and characterization of a therapeutic non-phospholipid liposomal nanocarrier with osteoinductive characteristics to promote bone formation[J]. ACS Nano, 2017, 11(8): 8055-8063.

[4] YU R, ZHANG HL, GUO BL. Conductive biomaterials as bioactive wound dressing for wound healing and skin tissue engineering[J]. Nano-Micro Letters, 2022, 14(1): 1.

[5] GRIFFIN DR, ARCHANG MM, KUAN CH, WEAVER WM, WEINSTEIN JS, FENG AC, RUCCIA A, SIDERIS E, RAGKOUSIS V, KOH J, PLIKUS MV, di CARLO D, SEGURA T, SCUMPIA PO. Activating an adaptive immune response from a hydrogel scaffold imparts regenerative wound healing[J]. Nature Materials, 2021, 20(4): 560-569.

[6] FAN C, XU Q, HAO RQ, WANG C, QUE YM, CHEN YX, YANG C, CHANG J. Multi-functional wound dressings based on silicate bioactive materials[J]. Biomaterials, 2022, 287: 121652.

[7] QIAO Y, YANG F, XIE TT, DU Z, ZHONG DN, QI YC, LI YY, LI WL, LU ZM, RAO JH, SUN Y, ZHOU M. Engineered algae: a novel oxygen-generating system for effective treatment of hypoxic cancer[J]. Science Advances, 2020, 6(21): eaba5996.

[8] ZHANG C, WU W, LI RQ, QIU WX, ZHUANG ZN, CHENG SX, ZHANG XZ. Peptide-based multifunctional nanomaterials for tumor imaging and therapy[J]. Advanced Functional Materials, 2018, 28(50): 1804492.

[9] PAN H, ZHENG MB, MA AQ, LIU LL, CAI LT. Cell/bacteria-based bioactive materials for cancer immune modulation and precision therapy[J]. Advanced Materials (Deerfield Beach, Fla), 2021, 33(50): e2100241.

[10] LI YN, GE J, LUO M, NIU W, LING XW, XU K, LIN C, LEI B, ZHANG XX. Elastomeric self-healing antibacterial bioactive nanocomposites scaffolds for treating skull defect[J]. Applied Materials Today, 2022, 26: 101254.

[11] 陈国强, 钟超. 生物材料创造可持续未来[J]. 合成生物学, 2022, 3(4): 617-620.
CHEN GQ, ZHONG C. Materials create a sustainable future[J]. Synthetic Biology Journal, 2022, 3(4): 617-620 (in Chinese).

[12] WANG YY, AN BL, XUE B, PU JH, ZHANG XL, HUANG YY, YU Y, CAO Y, ZHONG C. Living materials fabricated via gradient mineralization of light-inducible biofilms[J]. Nature Chemical Biology, 2021, 17(3): 351-359.

[13] WANG XY, ZHANG JC, LI K, AN BL, WANG YY, ZHONG C. Photocatalyst-mineralized biofilms as living bio-abiotic interfaces for single enzyme to whole-cell photocatalytic applications[J]. Science Advances, 2022, 8(18): eabm7665.

[14] HUANG JF, LIU SY, ZHANG C, WANG XY, PU JH, BA F, XUE S, YE HF, ZHAO TX, LI K, WANG YY, ZHANG JC, WANG LH, FAN CH, LU TK, ZHONG C. Programmable and printable *Bacillus subtilis* biofilms as engineered living materials[J]. Nature Chemical Biology, 2019, 15(1): 34-41.

[15] HAN W, ZHOU B, YANG K, XIONG X, LUAN SF, WANG Y, XU Z, LEI P, LUO ZS, GAO J, ZHAN YJ, CHEN GP, LIANG L, WANG R, LI S, XU H. Biofilm-inspired adhesive and antibacterial hydrogel with tough tissue integration performance for sealing hemostasis and wound healing[J]. Bioactive Materials, 2020, 5(4): 768-778.

[16] DURAJ-THATTE AM, MANJULA-BASAVANNA A, COURCHESNE NM D, CANNICI GI,

SÁNCHEZ-FERRER A, FRANK BP, HAG LV, COTTS SK, FAIRBROTHER DH, MEZZENGA R, JOSHI NS. Water-processable, biodegradable and coatable aquaplastic from engineered biofilms[J]. Nature Chemical Biology, 2021, 17(6): 732-738.

[17] LIU XY, YUK H, LIN ST, PARADA GA, TANG TC, THAM E, de la FUENTE-NUNEZ C, LU TK, ZHAO XH. 3D printing of living responsive materials and devices[J]. Advanced Materials (Deerfield Beach, Fla), 2018, 30(4): 1704821.

[18] LIU XY, TANG TC, THAM E, YUK H, LIN ST, LU TK, ZHAO XH. Stretchable living materials and devices with hydrogel-elastomer hybrids hosting programmed cells[J]. Proceedings of the National Academy of Sciences of the United States of America, 2017, 114(9): 2200-2205.

[19] WANG MQ, YANG YR, MIN JH, SONG Y, TU JB, MUKASA D, YE C, XU CH, HEFLIN N, McCUNE JS, HSIAI TK, LI ZP, GAO W. A wearable electrochemical biosensor for the monitoring of metabolites and nutrients[J]. Nature Biomedical Engineering, 2022, 6(11): 1225-1235.

[20] LIU XM, UEKI T, GAO HY, WOODARD TL, NEVIN KP, FU TD, FU S, SUN L, LOVLEY DR, YAO J. Microbial biofilms for electricity generation from water evaporation and power to wearables[J]. Nature Communications, 2022, 13: 4369.

[21] ZHANG C, HUANG JF, ZHANG JC, LIU SY, CUI MK, AN BL, WANG XY, PU JH, ZHAO TX, FAN CH, LU TK, ZHONG C. Engineered *Bacillus subtilis* biofilms as living glues[J]. Materials Today, 2019, 28: 40-48.

[22] LI YF, LI K, WANG XY, CUI MK, GE P, ZHANG JH, QIU F, ZHONG C. Conformable self-assembling amyloid protein coatings with genetically programmable functionality[J]. Science Advances, 2020, 6(21): eaba1425.

[23] AN BL, WANG YY, JIANG XY, MA CH, MIMEE M, MOSER F, LI K, WANG XY, TANG TC, HUANG YY, LIU Y, LU TK, ZHONG C. Programming living glue systems to perform autonomous mechanical repairs[J]. Matter, 2020, 3(6): 2080-2092.

[24] PU JH, LIU Y, ZHANG JC, AN BL, LI YF, WANG XY, DIN K, QIN C, LI K, CUI MK, LIU SY, HUANG YY, WANG YY, LV YN, HUANG JF, CUI ZQ, ZHAO SW, ZHONG C. Virus disinfection: virus disinfection from environmental water sources using living engineered biofilm materials (adv. sci. 14/2020)[J]. Advanced Science, 2020, 7(14): 2070076.

[25] PRAVESCHOTINUNT P, DURAJ-THATTE AM, GELFAT I, BAHL F, CHOU DB, JOSHI NS. Engineered *E. coli* Nissle 1917 for the delivery of matrix-tethered therapeutic domains to the gut[J]. Nature Communications, 2019, 10: 5580.

[26] LU YF, LI HS, WANG J, YAO MY, PENG Y, LIU TF, LI Z, LUO GX, DENG J. Engineering bacteria-activated multifunctionalized hydrogel for promoting diabetic wound healing[J]. Advanced Functional Materials, 2021, 31(48): 2105749.

[27] WANG XY, PU JH, LIU Y, BA F, CUI MK, LI K, XIE Y, NIE Y, MI QX, LI T, LIU LL, ZHU MZ, ZHONG C. Immobilization of functional nano-objects in living engineered bacterial biofilms for catalytic applications[J]. National Science Review, 2019, 6(5): 929-943.

[28] HARIMOTO T, HAHN J, CHEN YY, IM J, ZHANG J, HOU N, LI FD, COKER C, GRAY K, HARR N, CHOWDHURY S, PU K, NIMURA C, ARPAIA N, LEONG KW, DANINO T. A programmable encapsulation system improves delivery of therapeutic bacteria in mice[J]. Nature Biotechnology, 2022, 40(8): 1259-1269.

[29] CHEN BZ, KANG W, SUN J, ZHU RT, YU Y, XIA AG, YU M, WANG M, HAN JY, CHEN YX, TENG LJ, TIAN Q, YU Y, LI GL, YOU LC, LIU ZY, DAI ZJ. Programmable living assembly of materials by bacterial adhesion[J]. Nature Chemical Biology, 2022, 18(3): 289-294.

[30] GLASS DS, RIEDEL-KRUSE IH. A synthetic bacterial cell-cell adhesion toolbox for programming multicellular morphologies and patterns[J]. Cell, 2018, 174(3): 649-658.e16.

[31] PIÑERO-LAMBEA C, BODELÓN G, FERNÁNDEZ-PERIÁÑEZ R, CUESTA AM, ÁLVAREZ-VALLINA L, FERNÁNDEZ LÁ. Programming controlled adhesion of *E. coli* to target surfaces, cells, and tumors with synthetic adhesins[J]. ACS Synthetic Biology, 2015, 4(4): 463-473.

[32] TING SY, MARTÍNEZ-GARCÍA E, HUANG S, BERTOLLI SK, KELLY KA, CUTLER KJ, SU ED, ZHI H, TANG Q, RADEY MC, RAFFATELLU M, PETERSON SB, de LORENZO V, MOUGOUS JD. Targeted depletion of bacteria from mixed populations by programmable adhesion with antagonistic

competitor cells[J]. Cell Host & Microbe, 2020, 28(2): 313-321.e6.

[33] HATLEM D, TRUNK T, LINKE D, LEO JC. Catching a SPY: using the SpyCatcher-SpyTag and related systems for labeling and localizing bacterial proteins[J]. International Journal of Molecular Sciences, 2019, 20(9): 2129.

[34] CHEN TT, WANG KH, CHI X, ZHOU LZ, LI JJ, LIU LQ, ZHENG QB, WANG YB, YU H, GU Y, ZHANG J, LI SW, XIA NS. Construction of a bacterial surface display system based on outer membrane protein F[J]. Microbial Cell Factories, 2019, 18(1): 70.

[35] HAN CL, ZHANG XY, PANG GJ, ZHANG YY, PAN HZ, LI LY, CUI MH, LIU BN, KANG RR, XUE X, SUN T, LIU J, CHANG J, ZHAO PQ, WANG HJ. Hydrogel microcapsules containing engineered bacteria for sustained production and release of protein drugs[J]. Biomaterials, 2022, 287: 121619.

[36] HUSSAIN F, GUPTA C, HIRNING AJ, OTT W, MATTHEWS KS, JOSIC K, BENNETT MR. Engineered temperature compensation in a synthetic genetic clock[J]. Proceedings of the National Academy of Sciences of the United States of America, 2014, 111(3): 972-977.

[37] CUI MK, WANG XY, AN BL, ZHANG C, GUI XR, LI K, LI YF, GE P, ZHANG JH, LIU C, ZHONG C. Exploiting mammalian low-complexity domains for liquid-liquid phase separation-driven underwater adhesive coatings[J]. Science Advances, 2019, 5(8): eaax3155.

(本文责编 郝丽芳)